Appl. Phys. A (2016) 122:66
DOI 10.1007/s00339-016-9624-7

Applied Physics A
Materials Science & Processing

Breakdown field enhancement of Si-based MOS capacitor by post-deposition annealing of the reactive sputtered ZrO_xN_y gate oxide

Chun Chet Chew[1] · Kian Heng Goh[1] · Mohammad Saleh Gorji[1] · Chee Ghuan Tan[2] · S. Ramesh[1] · Yew Hoong Wong[1]

Received: 1 October 2015 / Accepted: 11 January 2016 / Published online: 21 January 2016

Abstract Zirconium oxynitride (ZrO_xN_y) thin films were deposited on silicon (100) substrates by radio frequency-reactive magnetron sputtering in an argon–oxygen–nitrogen atmosphere. Post-deposition annealing (PDA) process was performed in argon ambient at various annealing temperatures (500, 600, 700 and 800 °C) for 15 min. Metal–oxide–semiconductor capacitors were then fabricated with aluminum as the gate electrode. The effects of PDA process on the thin film's structural and electrical properties of the samples were investigated. The structural properties of the deposited films have been evaluated by atomic force microscopy, Fourier transform infrared spectroscopy and Raman spectroscopy. On the other hand, the electrical characterization of the film was conducted by current–voltage analysis. The Raman results revealed that (600–800 °C) annealed samples comprised of crystalline multiphase films (t-ZrO_2, fcc-ZrN and bcc γ-Zr_2ON_2). Interfacial layer consisted of Zr–Si–O, Si–O–N and Si–O phase was formed for all investigated samples, and interfacial layer growth was suppressed when annealed at lower temperatures (500 °C). Electrical result revealed that the sample annealed at a relatively low temperature of 500 °C has demonstrated the highest breakdown field which was attributed to the low surface roughness, the low interface trap and the highly amorphous multiphase film.

✉ Yew Hoong Wong
yhwong@um.edu.my

[1] Department of Mechanical Engineering, Faculty of Engineering, University of Malaya, 50603 Kuala Lumpur, Malaysia

[2] Department of Civil Engineering, Faculty of Engineering, University of Malaya, 50603 Kuala Lumpur, Malaysia

1 Introduction

Performance of semiconductor devices has increased dramatically over the last few decades. One of the major driving forces in evolving the electronics industry is its successful downscaling of the silicon (Si)-based metal–oxide semiconductor (MOS) devices' dimensions. However, the continual downscaling of MOS devices has led to the silicon dioxide (SiO_2) gate oxide thickness to be scaled down as well. As the thickness of oxide becomes less than 1.2 nm, the direct tunneling of electrons through the gate oxide due to leakage current will be very high [1]. Therefore, alternative materials with high dielectric constant (k) are required to replace SiO_2 as the gate dielectric. The requirements for choosing an alternative gate dielectric material are high dielectric constant, large bandgap, good thermodynamic stability and interface quality [1–3].

Zirconium oxide (ZrO_2) has been highlighted due to its high dielectric value (ranging from 22 to 25), its large bandgap energy (5.8–7.8 eV) [3] and being thermodynamically stable in contact with Si substrate. The large bandgap of ZrO_2 is sufficient to provide low gate leakage current which is essential in electrical properties of MOS capacitor devices. Unfortunately, the low-k interfacial layer (IL), which is not desirable as it effectively diminishes the capacitance of the MOS capacitor [4–6, 18]. As summarized in the previous works [4, 18], they have reported that the low-k interfacial layer (IL) is formed in oxygen ambient during oxidation process due to oxygen diffused into Si substrate. The IL thickness increases as the post-deposition annealing (PDA) temperature increases. Besides, crystallization temperature of gate dielectric layer can be increased and oxygen diffusion as well as impurities penetration through gate dielectrics can be reduced.

Based on the literature, a nitrogen-incorporated ZrO_2 film has shown encouraging improvement in detaining the growth of IL [1]. Two possible factors that attribute to this improvement are the passivation of the Si dangling bonds and that of the oxygen vacancies, which in turn reduces the interfacial traps and improves the thermal stability of the films [1]. The nitrogen-derived modification can be realized by the Si substrate treatment in N_2O and NH_3 gases prior to the deposition of ZrO_2 thin film [5] or the incorporation of nitrogen into the thin films during/after the deposition of ZrO_2 and the formation of Zr oxynitrides (ZrO_xN_y).

Different approaches and techniques have been used for the incorporation of nitrogen into the ZrO_2 thin films and formation of ZrO_xN_y on Si substrates. Some of the previously examined methods are ion plating [6], atomic layer deposition (ALD) [7], cathodic arc evaporation [8], filtered cathodic vacuum arc (FCVA) [9, 10], and the direct current (DC) [11–13] and radio frequency (RF) [14–17] magnetron sputtering. The latter is the most common method for the deposition of Zr_2O [3] and ZrO_xN_y thin films. Sputter deposition of ZrO_xN_y thin film can be realized by non-reactive and reactive approaches. In a typical non-reactive approach, Zr metal is sputtered onto the substrate in an inert gas ambient followed by the oxidation and nitridation process [4, 18, 19]. In the reactive approach, on the other hand, Zr metal can be sputtered in the presence of Ar and a mixture of reactive oxygen and nitrogen gases which would result in the formation of ZrO_xN_y thin films [11, 12, 14, 20–22]. For reactive approach, the ZrO_xN_y thin films can be formed in one time process which saves time and energy. The sputtered Zr atom reacts and combines with the O and N in the chamber and the ZrO_xN_y thin films deposited uniformly on Si substrate. Unreacted Zr atom can be suppressed to deposit on the substrates. [4, 18, 19]. There have also been some reports of two-stage reactive sputtering of ZrO_xN_y thin films: the first stage being the reactive sputtering of ZrN [2] or ZrO_2 [23] followed by the PDA process in oxygen or nitrogen-based environments, respectively. The substrate temperature can be controlled and fixed at the chamber environment temperature [24] or be elevated to higher temperatures [15] during the sputtering procedure based on the specific requirements.

It was previously shown that the simultaneous oxidation and nitridation of ZrO_2 in N_2O gas at the optimum 700 °C for 15 min greatly enhances the breakdown field of the Si-based MOS capacitor [17, 18, 25]. However, in order to reduce the PDA temperature and hence increase the energy and cost efficiency of the fabrication process, while maintaining the enhanced electrical properties, alternative approaches are required specifically for Si-based MOS capacitors. In this work, the reactive sputtering of ZrO_xN_y thin films on Si substrate was selected, manipulated and followed by the PDA process at various temperatures to meet the above-mentioned criteria. Based on the results, the optimum PDA temperature was achieved at 500 °C where the ZrO_xN_y gate oxide demonstrated the comparably high breakdown field value of 10.60 MV/cm at $J \sim 4.08 \times 10^{-6}$ A/cm^2.

2 Experimental

N–Si (100) substrates with dimension of (1 cm × 1 cm) were subjected to Radio Corporation of America (RCA) cleaning and treated with diluted HF solution to remove the native oxide from the surface. TF 450 radio frequency (RF)-reactive magnetron sputtering system was employed to deposit ZrO_xN_y thin film on top of the Si substrates in a high vacuum chamber with RF power of 170 W and working pressure of 3×10^{-5} mbar. When the desired pressure was reached, the Zr metal target was pre-sputtered for 2 min to remove the surface contaminants on the Zr target surface. Subsequently, Ar, O_2 and N_2 gases were purged into the chamber simultaneously. The flow rate of the gases was set at $f_{Ar}:f_{O2}:f_{N2} = 40:10:10$ SCCM. The 10 nm of ZrO_xN_y thin film was deposited which is measured and confirmed by the ellipsometer. The ZrO_xN_y samples (Fig. 1a) were placed in a horizontal tube furnace and heated up from room temperature to a set of various PDA temperatures (500–800 °C) in an Ar flow ambient. The heating rate was fixed at 10 °C/min. Once the set temperature was achieved, the temperature was held for 15 min. The furnace was cooled down to room temperature before the samples were taken out.

The effects of PDA process on the thin film's structural and electrical properties of the samples were investigated by various characterization techniques. Micro-Raman spectrometer (Horiba Xplora ONE) with an argon ion laser source (excitation wavelength of 514.5 nm) was used to detect molecular vibrational motions in the sample. The presence of chemical functional groups of the ZrO_xN_y thin

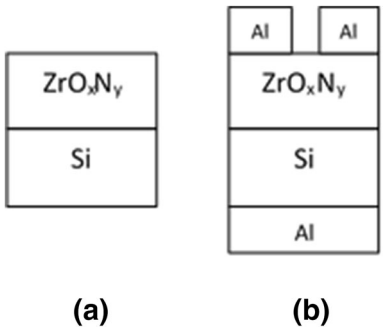

Fig. 1 **a** Sputtered ZrO_xN_y films on Si substrate, **b** Al metallization on top of ZrO_xN_y films and backside of Si substrate

films was identified by Fourier transform infrared (FTIR) (Perkin-Elmer Spectrum 400) with transmittance mode in the range of 1400–400 cm^{-1}. Atomic force microscope (AFM) (Ambios contact mode) was used to measure the root-mean-square (RMS) surface roughness and topography of the ZrO_xN_y thin films. Surface areas of 5 μm × 5 μm were scanned and then studied.

In order to characterize the electrical properties of the film, Al gate (Fig. 1b) was formed on the films by using Edwards Auto 360 thermal evaporator. A patterned metal mask with capacitor area of 0.2 cm^2 (0.2 cm × 1.0 cm) was aligned on top of the films. Al film was also deposited on the back side of Si substrate (Fig. 1b). Current–voltage (*I–V*) measurements were performed by using Keithley 236 source measure units (SMU). These measurements were done in sweep mode (from 0 to 15 V) at a frequency of 2 Hz.

3 Results and discussion

3.1 Raman analysis

Figure 2 demonstrates the Raman results of as-deposited and annealed ZrO_xN_y films on Si substrate at different temperatures (500–800 °C). For all the investigated samples, the sharp and strong peak at 520 cm^{-1} is strongly evident and it is the scattering from the Si substrate. A broad peak located at around 300 cm^{-1} originated also from the Si substrate. This information has been identified in our previous works reported in Ref. [4]. Besides, two peaks at 110 and 620 cm^{-1} are detected which are related to t-ZrO_2. Furthermore, an fcc-ZrN peak is present, located at around 220 cm^{-1} in the low-frequency region.

The most important information obtained from the Raman spectra is the detection of ZrO_xN_y band which is centered around 425 cm^{-1}. Based on the analysis reported by Pankaew et al. [26], bcc γ-Zr_2ON_2 phase is detected around 400–430 cm^{-1}. It is confirmed that ZrO_xN_y in our result corresponds to the bcc γ-Zr_2ON_2. When PDA temperature is raised to 600 °C, the amorphous ZrO_2, ZrN and Zr_2ON_2 grow to crystalline t-ZrO_2, fcc-ZrN and bcc γ-Zr_2ON_2 [26]. In addition, there is a peak located at 670 cm^{-1} which corresponds to Si–O vibration mode which assures the Si–O bond-related IL formation.

3.2 FTIR analysis

To further identify the chemical functional groups of the samples, FTIR analysis was carried out as a complementary method. Figure 3 displays the FTIR spectra of as-deposited and annealed ZrO_xN_y thin films on Si at different temperatures (500–800 °C) with transmittance spectra in 1400–400 cm^{-1} region. From the spectra, it can be observed that the transmittance peak appearing at 610 cm^{-1} originated from the Si–Si stretching vibration of Si substrate. This information has been identified in our previous works reported in Ref. [4]. There is no detectable peak of Zr–Zr or Zr–Si because of the inactive bond in the mid-infrared. The peak at 570 cm^{-1} is assigned to the Zr–O stretching vibration, typical of ZrO_2. This result confirms the existence of crystalline t-ZrO_2 in the film.

There is no transmission of Zr–N in the infrared region because of the metallic behavior of ZrN structure. Besides that, the weak transmittance band at around 740 cm^{-1} corresponds to Zr–O–Si vibrational modes which imply the formation of $ZrSiO_x$ and/or $ZrSiO_xN_y$ as the IL. Moreover,

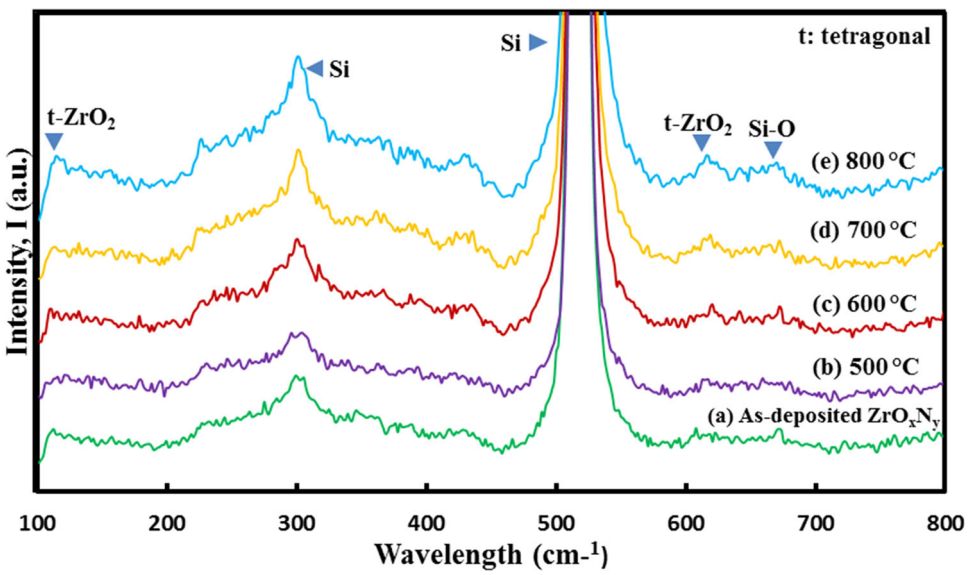

Fig. 2 Raman spectra of as-deposited and annealed ZrO_xN_y films at various temperatures (500–800 °C) on Si substrate

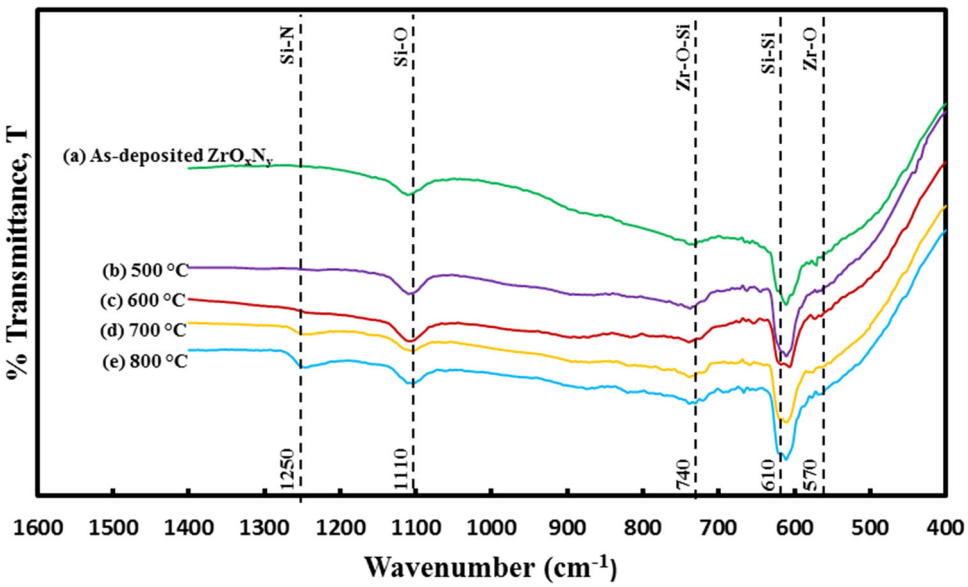

Fig. 3 FTIR transmittance spectra of as-deposited and annealed ZrO_xN_y films at various temperatures (500–800 °C) on Si substrate

the transmittance band at 1110 cm^{-1} is related to the Si–O bond in SiO_x, Si–O–N vibration and/or Zr–O–Si vibration. During deposition, reactive oxygen and nitrogen species in the plasma not only react with Zr atoms, they also diffuse to the silicon surface and an interface formed owing to their small size and high energy. Furthermore, the Si–N stretching vibration corresponds to 1250 cm^{-1} peak [27]. A weak broad transmittance band is observed at temperature 700 °C, and the intensity of Si–N transmittance band increased when annealed up to 800 °C. Si–N compound may be formed by reconstructed Si–O–N compound since the Si–N compound has higher thermal stability when heated at 700 °C for 15 min according to the analysis by [4]. Another report by Chai et al. [28] indicates that Si_3N_4 is formed through the migration of N atom when annealed at high temperatures. Oxygen is trapped at the interface as trapped charged.

3.3 AFM analysis

Figure 4 shows the RMS surface roughness value of as-deposited (0.63 nm) and annealed ZrO_xN_y films at various temperatures (500–800 °C) on Si substrate. The RMS surface roughness decreases from 0.63 to 0.37 nm and then increases to 1.28 nm when the samples are post-deposition annealed from 500 to 800 °C. As-deposited sample's surface roughness is attributed to the formed IL, while the 500 °C annealed sample has smoothest surface with RMS roughness value of 0.37 nm. Although a very small amount of grains have been formed on the surface of the sample, PDA at high temperature consolidates the grains. The aggressive and rapid grain formation at higher temperature may be due to grain clustering under high activation energy. Besides, densification of the film decreases the development of IL. Similar phenomenon is also reported at Atuchin et al. work [31]. It has been shown that as the thickness of the IL decreases the density of the interfacial trap density decreases as well [18]. The reduction in the interfacial trap density has been attributed to the incorporation of the nitrogen [18], as is the case in this study, and has direct effect on the electrical properties of the thin film.

The surface of the sample becomes rougher with RMS surface roughness of 0.58 nm when being post-deposition annealed at 600 °C as the amorphous ZrO_2, ZrN and Zr_2ON_2 grow to crystalline t-ZrO_2, fcc-ZrN and bcc γ-Zr_2ON_2, respectively. The RMS surface roughness value increases from 0.73 to 1.28 nm as the PDA temperature increases from 700 to 800 °C due to the continual growth of grains. This result is similar to the result of Chen et al. [29], in which the surface of Sm_2O_3 film was non-uniform and rough after annealing at high temperatures. In the following section, it is shown that the smoothness of the 500 °C annealed sample and the resulting densification of the ZrO_xN_y thin film and the limitation of IL development yield in an enhanced electric field in the corresponding MOS–capacitor device.

3.4 Electrical (*I–V*) analysis

The leakage current density–electric field (*J–E*) characteristics of investigated samples are shown in Fig. 5. *J–E* characteristics are transformed from the current–voltage (*I–V*) measurements based on the following relationships [30]:

$$J = I/A_C \quad \text{and} \quad E = \left(V_g - V_{FB}\right)/t, \tag{1}$$

where A_C is the capacitor area, V_g is the gate voltage, V_{FB} is the flat-band voltage, and t is the thickness of thin film.

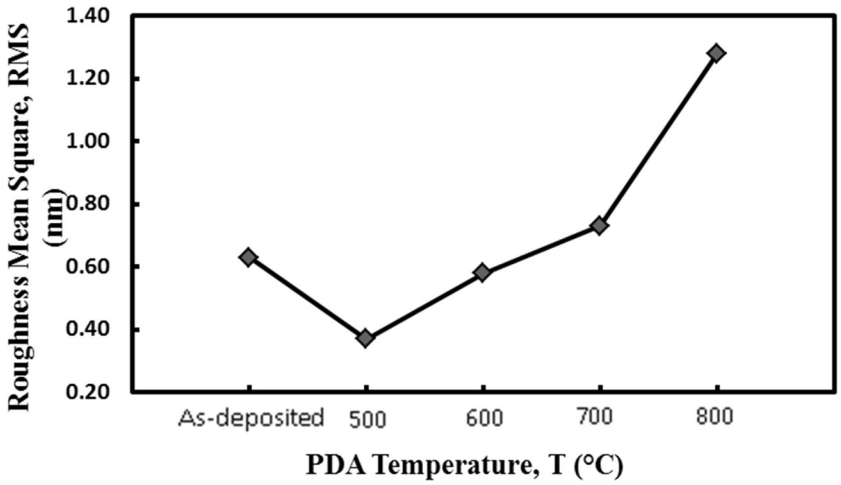

Fig. 4 The RMS surface roughness of as-deposited and annealed samples at various temperatures (500–800 °C)

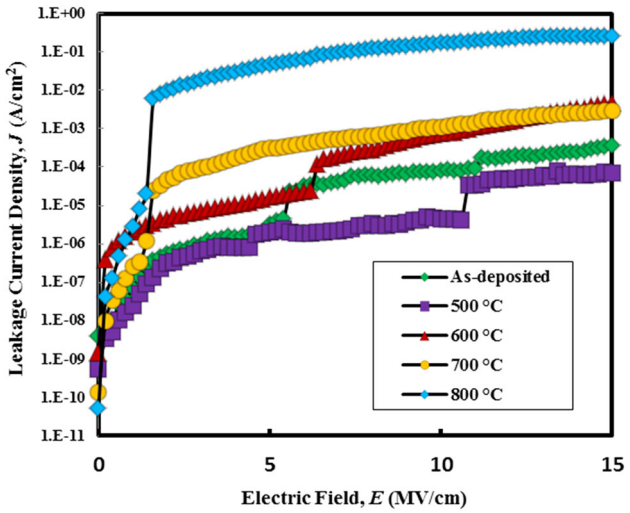

Fig. 5 *J–E* characteristics of as-deposited and annealed ZrO_xN_y films at various temperatures (500–800 °C) on Si substrate

It is indicated in Fig. 5 that the as-deposited characterized MOS capacitor possessed one dielectric breakdown, whereas samples annealed at (500–800 °C) revealed two dielectric breakdowns for all characterized MOS capacitors. Dielectric breakdown is defined as the instantaneous increment of leakage current density that causes the electrical breakdown of dielectric at a specific electric field. If the breakdown of both layers (ZrO_xN_y and IL) occurs at the same leakage current density, the *I–V* analyzer records one-step breakdown. When one layer is broken down, the applied electric field is then imposed on the second layer. The electric field will be increased until the second layer breakdown happens and the two-step breakdown will be recorded [30].

Both of the samples annealed at 700 and 800 °C possess the lowest dielectric breakdown of 1.40 MV/cm at $J \sim 1.20 \times 10^{-6}$ A/cm^2 and $J \sim 2.05 \times 10^{-5}$ A/cm^2, respectively, due to film crystallization which creates path for the leakage current to tunnel through the grain boundary to the film and IL. On the other hand, the 500 °C annealed sample possesses the highest dielectric breakdown of 10.60 MV/cm at $J \sim 4.08 \times 10^{-6}$ A/cm^2. The highest dielectric breakdown in the 500 °C annealed sample is attributed to the amorphous structure of multiphase film, the lowest surface roughness value as well as lowest interface trap.

4 Conclusions

In conclusion, ZrO_xN_y thin films were successfully deposited on Si substrate by employing RF-reactive magnetron sputtering technique. Structural and electrical properties of post-deposition annealed ZrO_xN_y thin films on Si substrate at various temperatures (500–800 °C) and fixed duration of 15 min were presented. Raman analysis indicated that there was crystalline growth when the PDA temperature increased. Multiphase films (t-ZrO_2, fcc-ZrN and bcc γ-Zr_2ON_2) were formed. FTIR analysis indicated that Zr–O, Zr–O–Si, Si–O compounds were formed in all investigated samples. Zr–O–Si and Si–O vibrations implied the formation IL, and it was suppressed when annealed at various temperatures. AFM analysis indicated that the 500 °C annealed sample has the lowest RMS surface roughness value of 0.37 due to the consolidation of grains and densification of film. From the electrical characterization, it was verified that 500 °C annealed sample possessed the highest dielectric breakdown of 10.60 MV/cm at $J \sim 4.08 \times 10^{-6}$ A/cm^2 which was attributed to the amorphous structure of multiphase film, lowest surface roughness value as well as lowest interface trap.

Acknowledgments The authors gratefully acknowledge the financial support provided by University of Malaya Research Grant

(UMRG) Programme (Project No. RP024A-13AET), Ministry of Education Malaysia through Fundamental Research Grant Scheme (Project No. FP010B-2013B) and Ministry of Sains, Technology and Innovation (MOSTI) Malaysia through Science Fund (Project No. SF011-2015).

References

1. R. De Almeida, I.J.R. Baumvol, Surf. Sci. Rep. **49**, 1 (2003)
2. R.E. Nieh, C.S. Kang, H.-J. Cho, K. Onishi, R. Choi, S. Krishnan, J.H. Han, Y.-H. Kim, M.S. Akbar, J.C. Lee, IEEE Trans. Electron Devices **50**, 333 (2003)
3. Y.H. Wong, K.Y. Cheong, J. Mater. Sci. Mater. Electron. **21**, 980 (2010)
4. Y.H. Wong, K.Y. Cheong, J. Alloys Compd. **509**, 8728 (2011)
5. L.-M. Chen, Y.-S. Lai, J. Chen, Thin Solid Films **515**, 3724 (2007)
6. J.-H. Huang, T.-H. Wu, G.-P. Yu, Surf. Coat. Technol. **203**, 3491 (2009)
7. W. Weinreich, V. Ignatova, L. Wilde, S. Teichert, M. Lemberger, A. Bauer, R. Reiche, E. Erben, J. Heitmann, L. Oberbeck, J. Appl. Phys. **106**, 4107 (2009)
8. M. Laurikaitis, J. Dudonis, D. Milčius, Thin Solid Films **516**, 1549 (2008)
9. Y.-M. Chen, B. Liao, X.-Y. Wu, H.-X. Zhang, X. Zhang, Surf. Coat. Technol. **228**, S210 (2013)
10. Y. Chen, H. Zhang, Z. Li, W. Cao, B. Liao, X. Zhang, Surf. Eng. **29**, 567 (2013)
11. P. Carvalho, J.-M. Chappé, L. Cunha, S. Lanceros-Méndez, P. Alpuim, F. Vaz, E. Alves, C. Rousselot, J. Espinós, A. González-Elipe, J. Appl. Phys. **103**, 104907 (2008)
12. S. Mohamed, A.A. El-Rahman, M.R. Ahmed, J. Phys. D Appl. Phys. **40**, 7057 (2007)
13. M.-H. Chan, P.-L. Wu, F.-H. Lu, Thin Solid Films **518**, 7300 (2010)
14. S.K. Rawal, A.K. Chawla, V. Chawla, R. Jayaganthan, R. Chandra, Mater. Sci. Eng. B **172**, 259 (2010)
15. A. Rizzo, M. Signore, L. Mirenghi, E. Piscopiello, L. Tapfer, J. Phys. D Appl. Phys. **42**, 235401 (2009)
16. J.-X. Chen, J.-P. Xu, L. Liu, P.-T. Lai, Appl. Phys. Express **6**, 084202 (2013)
17. Y.H. Wong, K.Y. Cheong, Ceram. Int. **39**, S475 (2013)
18. Y.H. Wong, K.Y. Cheong, J. Electrochem. Soc. **158**, H1270 (2011)
19. Y.H. Wong, V. Atuchin, V. Kruchinin, K.Y. Cheong, Appl. Phys. A **115**, 1069 (2014)
20. Y.-H. Wu, L.-L. Chen, J.-R. Wu, M.-L. Wu, C.-C. Lin, C.-H. Chang, IEEE Electron Device Lett. **31**, 1008 (2010)
21. S. Venkataraj, O. Kappertz, R. Jayavel, M. Wuttig, J. Appl. Phys. **92**, 2461 (2002)
22. S.K. Rawal, A.K. Chawla, R. Jayaganthan, R. Chandra, Mater. Sci. Eng. B **181**, 16 (2014)
23. S. Jeon, C.-J. Choi, T.-Y. Seong, H. Hwang, Appl. Phys. Lett. **79**, 245 (2001)
24. A. Rizzo, M. Signore, L. Mirenghi, T. Di Luccio, Thin Solid Films **517**, 5956 (2009)
25. Y.H. Wong, K.Y. Cheong, Nanoscale Res. Lett. **6**, 1 (2011)
26. P. Pankaew, T. Rattana, S. Chaiyakun, P. Limsuwan, P. Klumdoung, J. Appl. Sci. Res. **9**, 6103 (2013)
27. L. Saci, R. Mahamdi, F. Mansour, P. Temple-Boyer, E. Scheid, Influence of the annealing condition on the BN bonds intensity detected by FTIR characterization, in: *2011 7th International Conference on Electrical and Electronics Engineering (ELECO)* (IEEE, 2011), p. 2
28. J. Chai, J. Pan, Z. Zhang, S. Wang, Q. Chen, C. Huan, Appl. Phys. Lett. **92**, 092119 (2008)
29. F.-H. Chen, M.-N. Hung, J.-F. Yang, S.-Y. Kuo, J.-L. Her, Y.H. Matsuda, T.-M. Pan, J. Phys. Chem. Solids **74**, 570 (2013)
30. T. Kurniawan, K.Y. Cheong, K.A. Razak, Z. Lockman, N. Ahmad, J. Mater. Sci. Mater. Electron. **22**, 143 (2011)
31. V.V. Atuchin, V.N. Kruchinin, Y.H. Wong, K.Y. Cheong, Mater. Lett. **105**, 72–75 (2013)